



GaN electronic devices

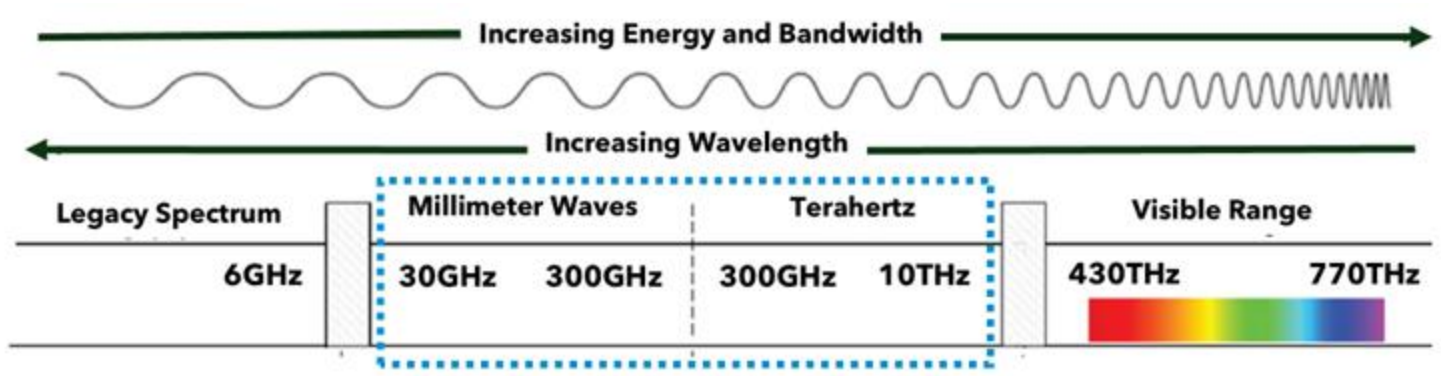
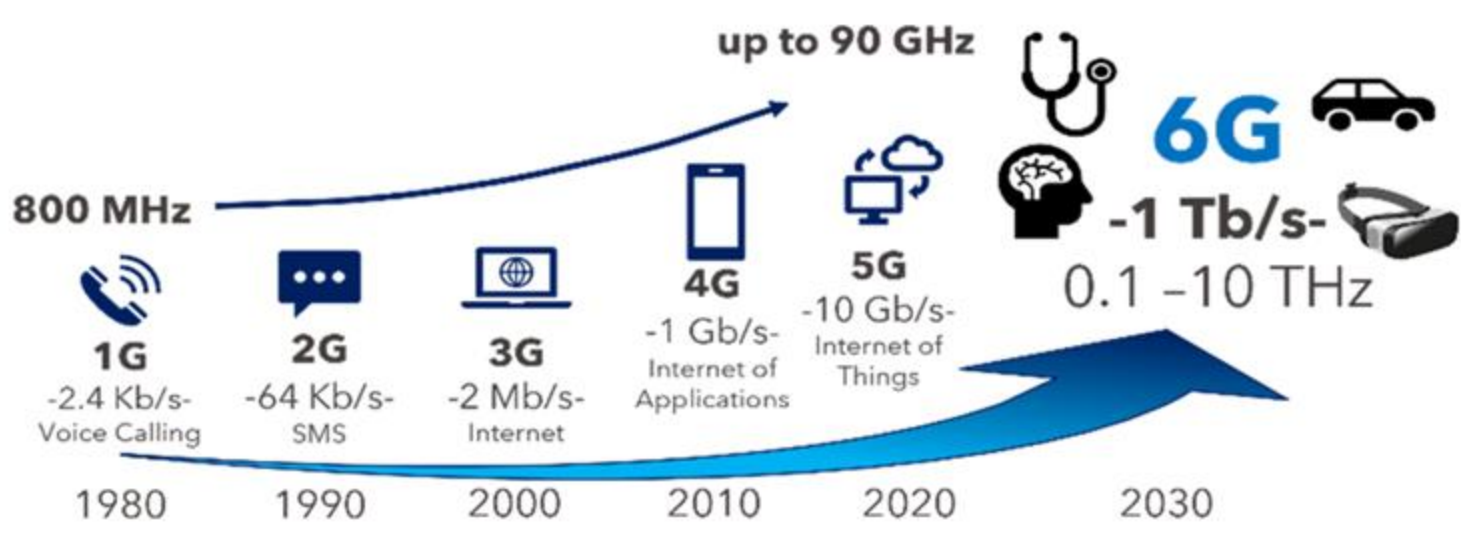
Elison Matioli

Institute of Electrical and Micro-engineering

Power and Wide-band-gap Electronics Research (POWERlab)

Ecole Polytechnique Fédérale de Lausanne (EPFL), Switzerland

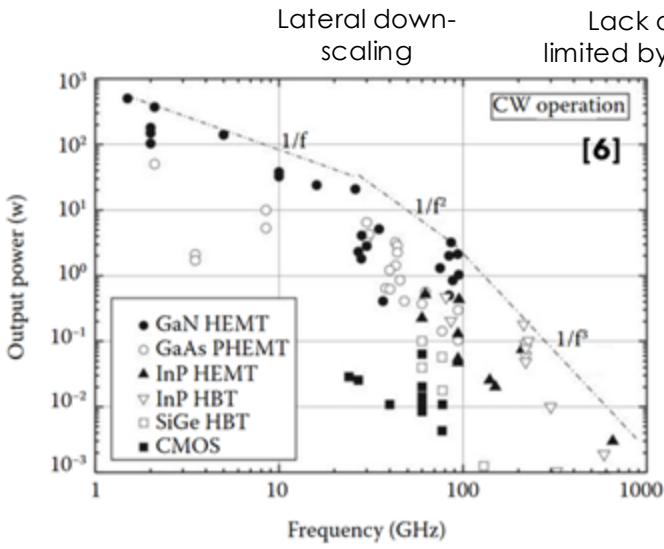
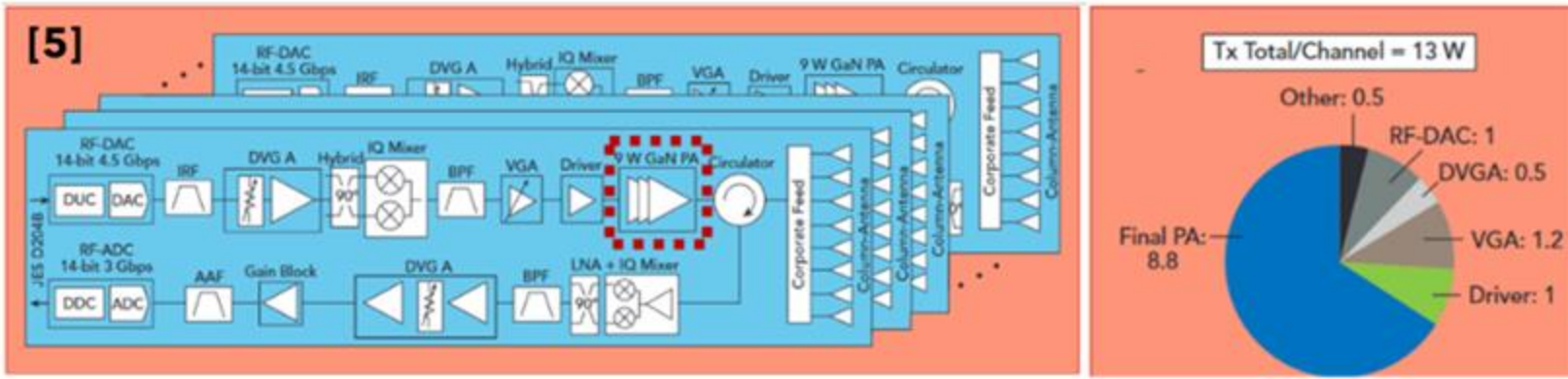
Lateral radio frequency (RF) devices



[1] E. A. Kadir, R. Shubak, S. K. Abdul Rahim, M. Himdi, M. R. Kamarudin, and S. L. Rosa, "BSG and 6G: Next Generation Wireless Communications Technologies, Demand and Challenges," in 2021 International Congress of Advanced Technology and Engineering (ICOTEN), Jul. 2021, pp. 1-6, doi: 10.1109/ICOTENS2080.2021.9493470.

[2] T. Nagatsuma, "Terahertz Technologies: Present and Future," IEICE Electronics Express, vol. 8, no. 14, pp. 1127-1142, 2011, doi:10.1587/elex.8.1127

Efficiency of power amplifiers dominate



Challenge: Achieving high-output power at mmWave band

[3] N. Cahoon, P. Srinivasan, and F. Guarin,
[5] B. Peterson, D. Schnauffer
[6] K. Shinohara "GaN-HEMT Scaling Technologies for High Frequency Radio Frequency and Mixed Signal Applications"

Material Properties of Microwave Semiconductors

	Si	InP	GaAs	SiC	InN	GaN	AlN
Egap (eV)	1.1	1.34	1.43	3.3 (4H)	0.63	3.4	6.1
Electron mobility (cm ² /V·s)	1,350	12,000*	8,500*	900	3,300	2,000*	1,100
2DEG density (×10 ¹³ cm ⁻²)	N/A	0.3*	<0.2	N/A	N/A	>2	N/A
Electron effective mass	0.26	0.08	0.067	0.29	0.11	0.2	0.4
Saturation velocity (×10 ⁷ cm/s)	1	3.3	1	2	3.5	1.5–2.5	1.5
Critical electric field (MV/cm)	0.3	0.5	0.4	3	1	3.3	6–15
Thermal conductivity (W/cm·K)	1.3	0.7	0.5	4.9	1.2	2	2
Relative dielectric constant	12	12.5	13	9.8	15.3	9.5	9

* Measured on InAlAs/InGaAs, AlGaAs/InGaAs, AlGaN/GaN HEMT structures.

III_Nitrides: Unique combination of high breakdown field, high electron velocity, and large sheet electron densities offers simultaneous high bandwidth and breakdown voltage.

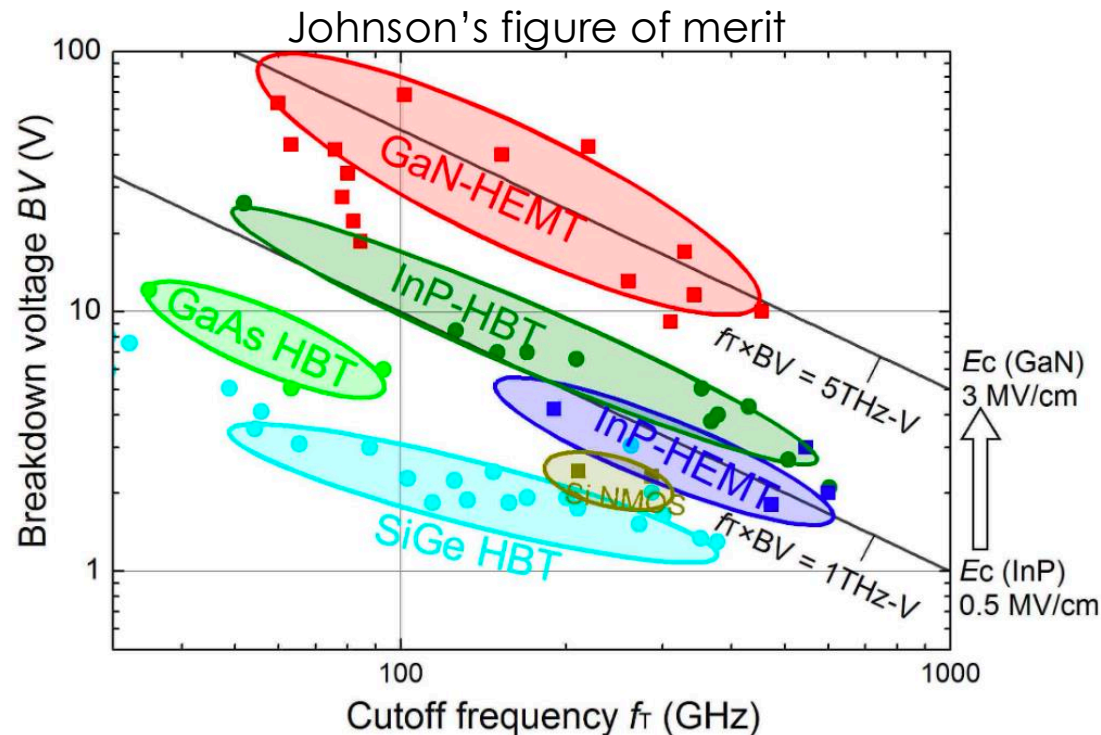
Thermal characteristics are enhanced using high thermal conductivity SiC substrates.

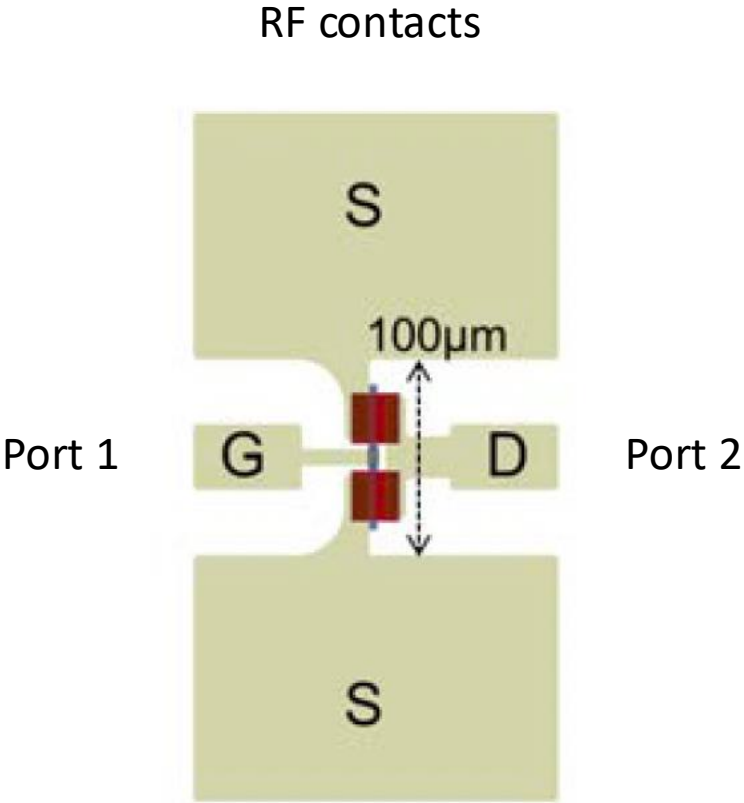
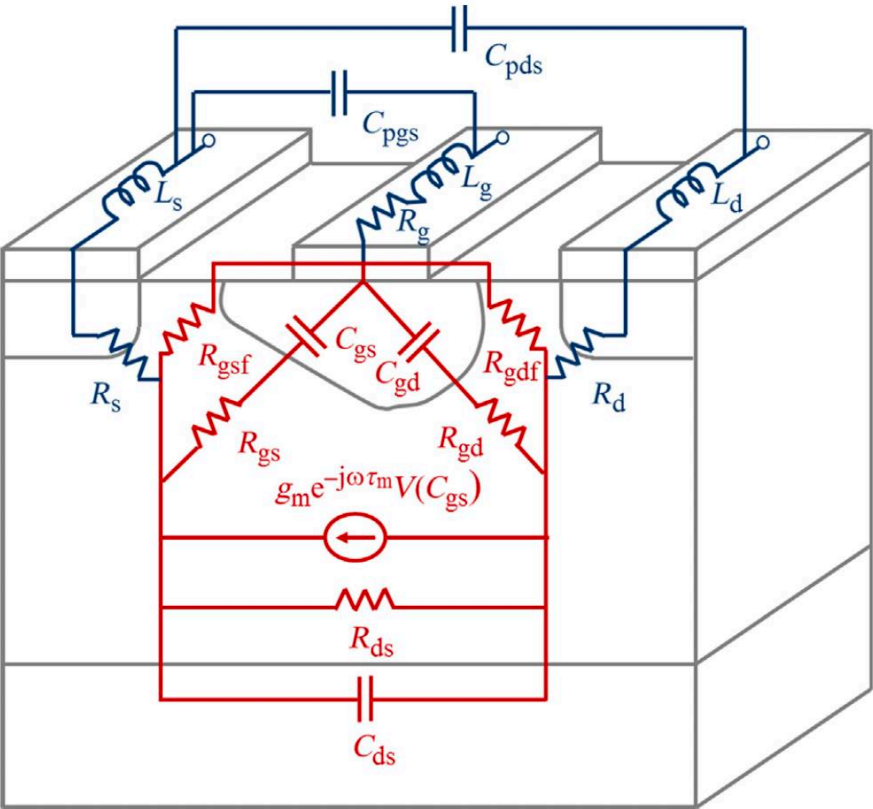
GaN HEMTs enable power amplifiers (PAs) with high power added efficiency, significantly higher output power and power density than in GaAs or InP.

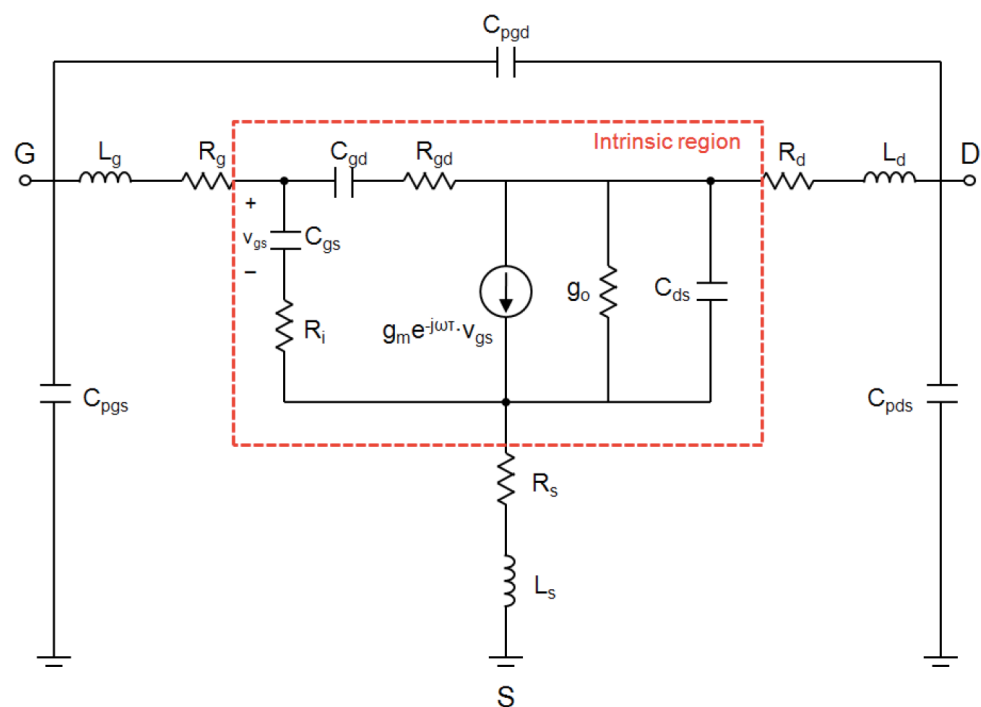
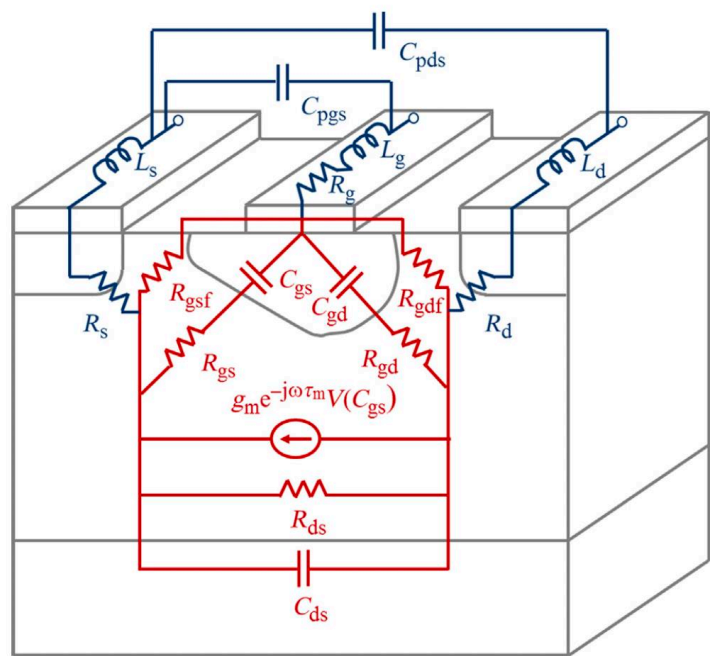
For RF and mixed-signal applications:

f_T , f_{max} , maximum drain current and breakdown voltage (BV) are key device performance parameters.

Device scaling successfully increases f_T and f_{max} of GaN transistors but simultaneously deteriorated BV due small dimension. Low BV greatly restricts the dynamic range of the circuit and represents a severe limitation.





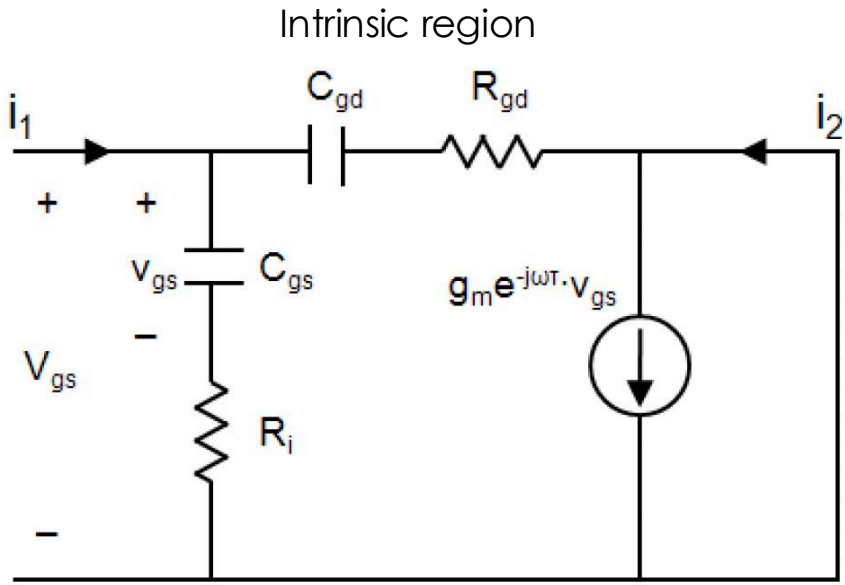
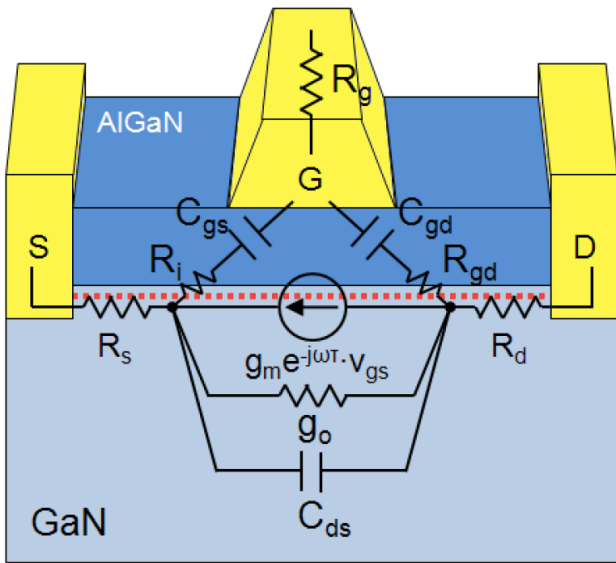


$$g_m = \left. \frac{dI_{DS}}{dV_{GS}} \right|_{V_{DS}=const.}$$

$$g_o = \left. \frac{dI_{DS}}{dV_{DS}} \right|_{V_{GS}=const.}$$

When the variation of V_{GS} is too fast, I_{DS} cannot be changed immediately since it takes time to charge or discharge C_g (tau is the g_m delay)

$$g_m(\omega) = g_m e^{-j\omega\tau}$$

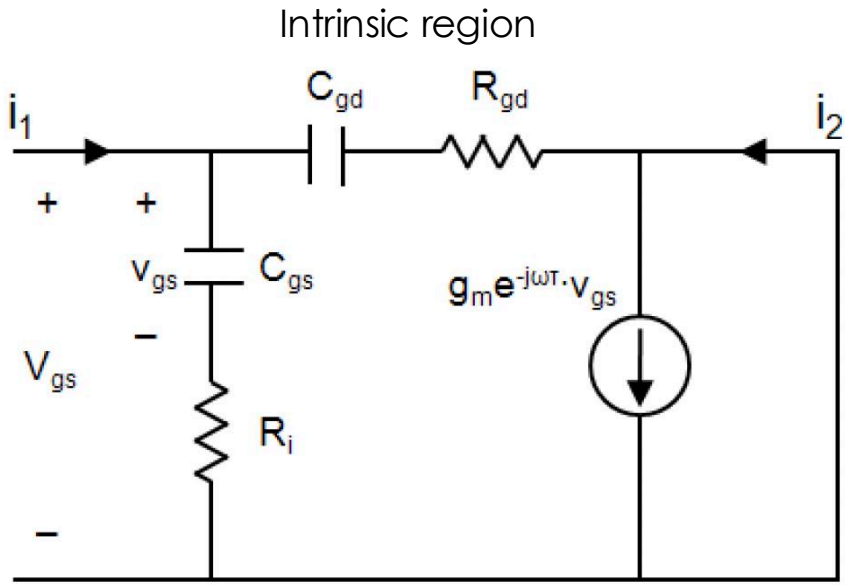
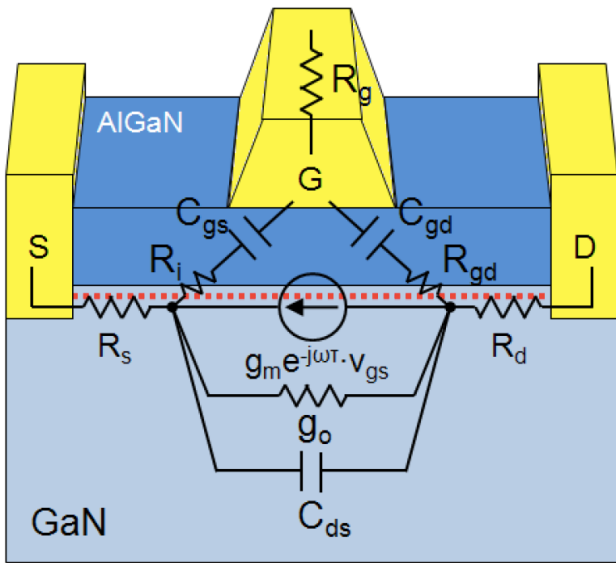


At the current-gain cutoff frequency f_T , the magnitude of current gain equals unity ($|h_{21}| = |i_2 / i_1| = 1$) with the output short-circuited

$$A_I|_{r_L=0} = \frac{i_d}{i_g} \Big|_{r_L=0} \rightarrow A_I(f_T)|_{r_L=0} = 1 \rightarrow$$
$$i_1 = \frac{V_{gs}}{\frac{1}{j\omega C_{gs}} + R_i} + \frac{V_{gs}}{\frac{1}{j\omega C_{gd}} + R_{gd}}$$
$$i_2 = g_m e^{-j\omega\tau} v_{gs} = g_m e^{-j\omega\tau} \frac{1}{\frac{1}{j\omega C_{gs}} + R_i} V_{gs}$$

$$|h_{21}| = \left| \frac{i_2}{i_1} \right| = \left| \frac{(1 + j\omega R_{gd} C_{gd}) g_m e^{-j\omega\tau}}{j\omega (C_{gs} + C_{gd}) - \omega^2 C_{gs} C_{gd} (R_i + R_{gd})} \right| \cong \frac{g_m}{2\pi f (C_{gs} + C_{gd})}$$

term $\omega R_{gd} C_{gd}$ is typically much less than unity and $\omega (C_{gs} + C_{gd}) \gg \omega^2 C_{gs} C_{gd} (R_i + R_{gd})$



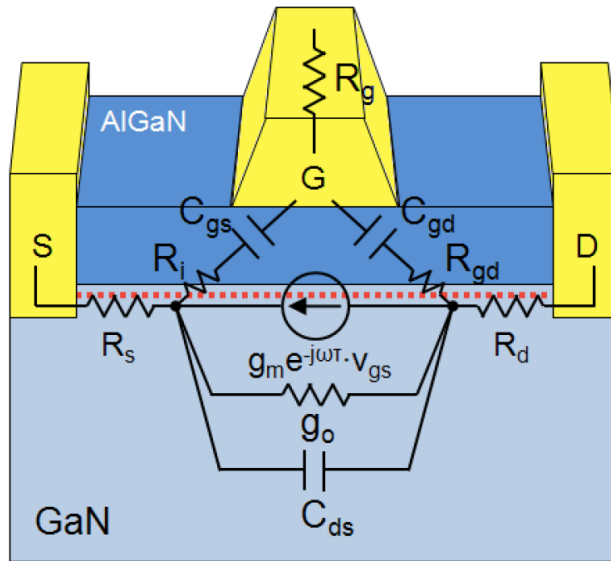
In short gate length devices, an alternative expression for f_T , with a more direct physical meaning, can be written by substituting $g_m = v_{sat}(C_{gs}+C_{gd})/L_g$

$$f_T = \frac{v_{sat}}{2\pi L_g}$$

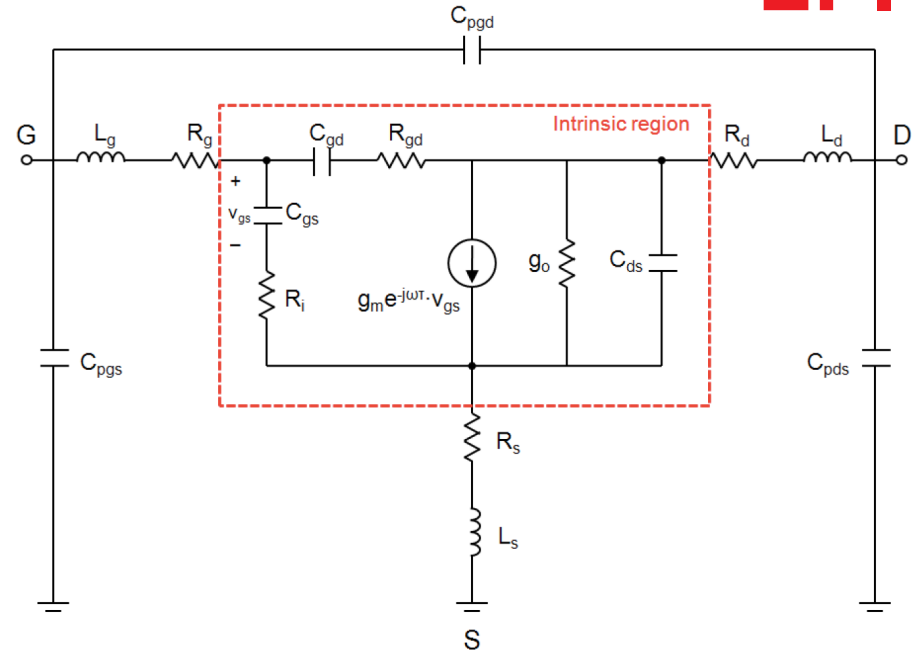
Considering extrinsic circuit elements such as R_s , R_d , and g_o :

$$f_T = \frac{g_m}{2\pi(C_{gs} + C_{gd})(1 + (R_s + R_d)g_o) + g_m C_{gd}(R_s + R_d)}$$

Principles of high frequency devices



W. Chung, MIT thesis, 2011



f_T is the frequency at which the magnitude of short-circuit current gain equals unity (or 0 dB)

- f_T is the frequency at which A_I goes to unity when the output is shorted to the ground

$$A_I|_{r_L=0} = \frac{I_d}{I_g} \Big|_{r_L=0} \rightarrow A_I(f_T)|_{r_L=0} = 1 \rightarrow f_T = \frac{g_m}{2\pi(C_{gs} + C_{gd})(1 + (R_s + R_d)g_o) + g_m C_{gd}(R_s + R_d)}$$

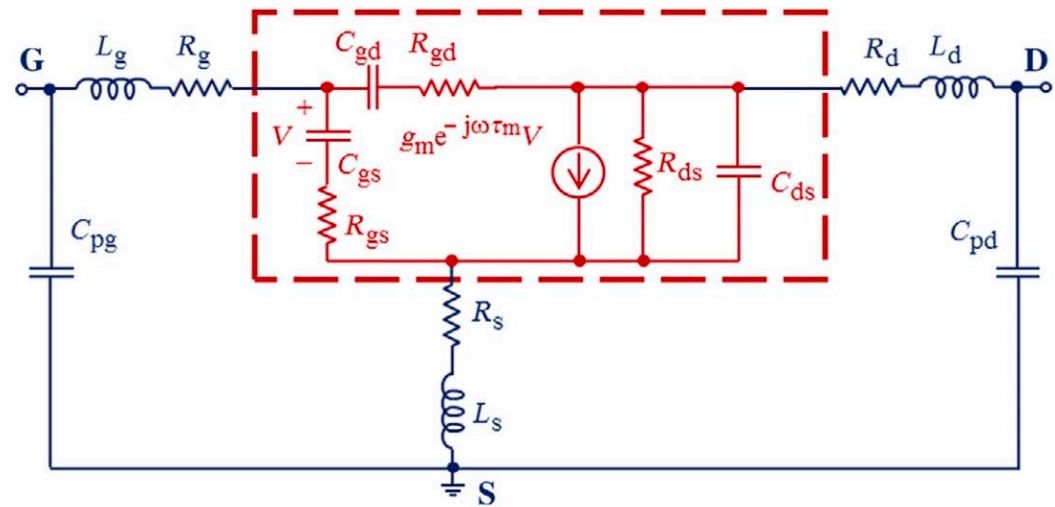
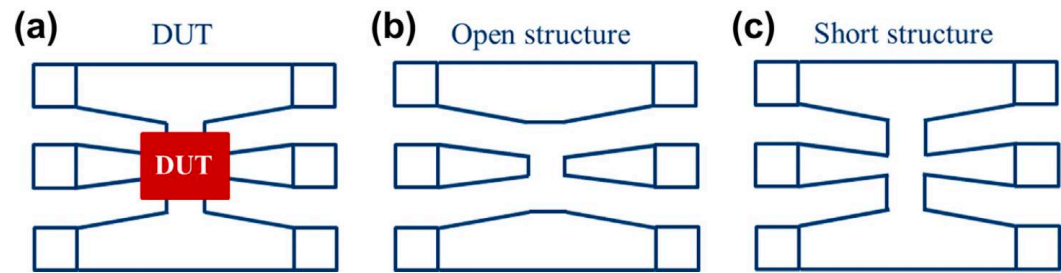
f_{max} is the frequency at which the unilateral power gain equals unity (or 0 dB)

- f_{max} is the frequency at which A_P goes to unity when the input/source and output/load are matched conjugately

$$A_P(f_{max}) \Big|_{z_s=z_{in}^* \text{ \& \; } z_L=z_{out}^*} = 1 \rightarrow f_{max} \cong \frac{f_T}{2\sqrt{(R_i + R_s + R_g)g_o + (2\pi f_T)R_g C_{gd}}}$$

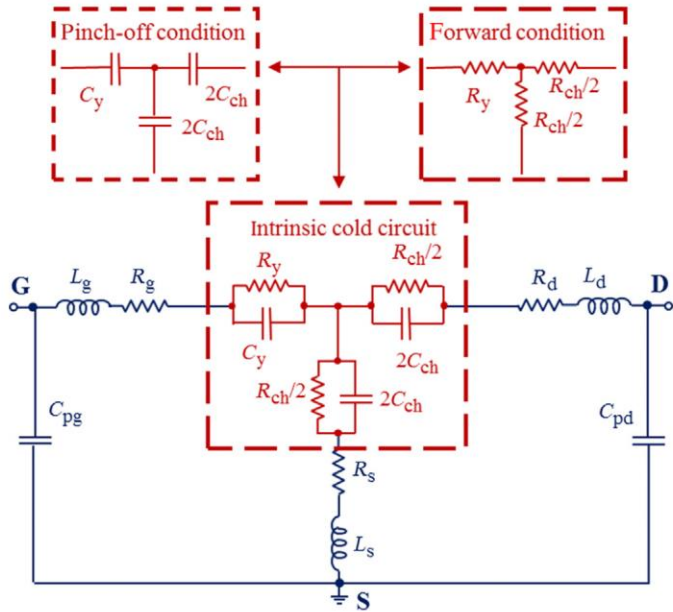
Optimization of f_{MAX} relies on the maximizing f_T and reduction of R_i , R_s , R_g , C_{gd} , and g_o

De-embedding the pads to retrieve the intrinsic device components



Measuring high frequency devices

Different bias conditions can be used to reveal different circuit elements



$$Y_{11} = \frac{1}{R_{gs} + \frac{1}{j\omega C_{gs}}} + \frac{1}{R_{gd} + \frac{1}{j\omega C_{gd}}}$$

$$= \frac{\omega^2 R_{gs} C_{gs}^2}{1 + \omega^2 R_{gs}^2 C_{gs}^2} + \frac{\omega^2 R_{gd} C_{gd}^2}{1 + \omega^2 R_{gd}^2 C_{gd}^2} + j\omega \left(\frac{C_{gs}}{1 + \omega^2 R_{gs}^2 C_{gs}^2} + \frac{C_{gd}}{1 + \omega^2 R_{gd}^2 C_{gd}^2} \right)$$

$$Y_{21} = \frac{\frac{g_m e^{-j\omega\tau_m}}{j\omega C_{gs}}}{R_{gs} + \frac{1}{j\omega C_{gs}}} - \frac{1}{R_{gd} + \frac{1}{j\omega C_{gd}}} = \frac{g_m [\cos(\omega\tau_m) - \sin(\omega\tau_m)\omega R_{gs} C_{gs}]}{1 + \omega^2 R_{gs}^2 C_{gs}^2} +$$

$$- \frac{\omega^2 R_{gd} C_{gd}^2}{1 + \omega^2 R_{gd}^2 C_{gd}^2} - j \left\{ \frac{g_m [\cos(\omega\tau_m)\omega R_{gs} C_{gs} + \sin(\omega\tau_m)]}{1 + \omega^2 R_{gs}^2 C_{gs}^2} + \frac{\omega C_{gd}}{1 + \omega^2 R_{gd}^2 C_{gd}^2} \right\}$$

$$Y_{12} = -\frac{1}{R_{gd} + \frac{1}{j\omega C_{gd}}}$$

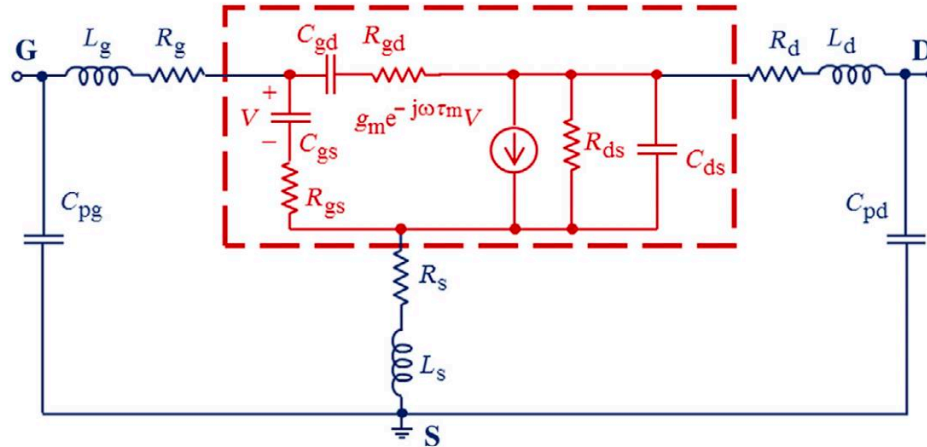
$$= -\frac{\omega^2 R_{gd} C_{gd}^2}{1 + \omega^2 R_{gd}^2 C_{gd}^2} - \frac{j\omega C_{gd}}{1 + \omega^2 R_{gd}^2 C_{gd}^2}$$

$$Y_{22} = g_{ds} + j\omega C_{ds} + \frac{1}{R_{gd} + \frac{1}{j\omega C_{gd}}}$$

$$= g_{ds} + \frac{\omega^2 R_{gd} C_{gd}^2}{1 + \omega^2 R_{gd}^2 C_{gd}^2} + j\omega \left(C_{ds} + \frac{C_{gd}}{1 + \omega^2 R_{gd}^2 C_{gd}^2} \right)$$

Measuring high frequency devices

All small signal intrinsic elements can be retrieved



$$R_{gd} = -\operatorname{Re}\left(\frac{1}{Y_{12}}\right)$$

$$C_{gd} = \frac{1}{\omega \operatorname{Im}\left(\frac{1}{Y_{12}}\right)}$$

$$R_{gs} = \operatorname{Re}\left(\frac{1}{Y_{11} + Y_{12}}\right)$$

$$C_{gs} = -\frac{1}{\omega \operatorname{Im}\left(\frac{1}{Y_{11} + Y_{12}}\right)}$$

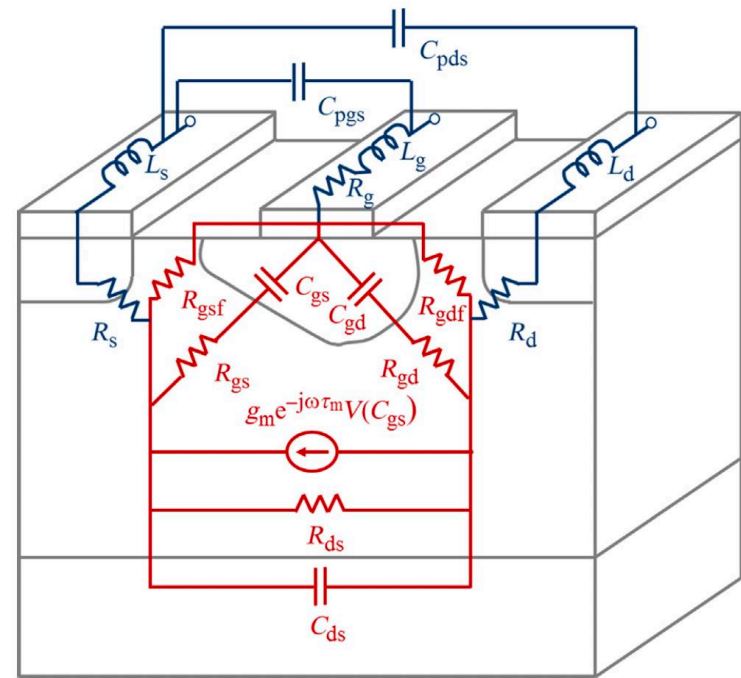
$$R_{ds} = \frac{1}{\operatorname{Re}(Y_{22} + Y_{12})}$$

$$C_{ds} = \frac{\operatorname{Im}(Y_{22} + Y_{12})}{\omega}$$

$$g_m = \left| \frac{(Y_{11} + Y_{12})(Y_{21} - Y_{12})}{\operatorname{Im}(Y_{11} + Y_{12})} \right|$$

$$\tau_m = -\frac{1}{\omega} \operatorname{phase} \left\{ (Y_{21} - Y_{12}) \left[1 + j \frac{\operatorname{Re}(Y_{11} + Y_{12})}{\operatorname{Im}(Y_{11} + Y_{12})} \right] \right\}$$

Y parameters (admittance matrix) are connected to physical device parameters, but it is difficult to measure voltages and currents



$$\begin{bmatrix} i_1 \\ i_2 \end{bmatrix} = \begin{bmatrix} y_{11} & y_{12} \\ y_{21} & y_{22} \end{bmatrix} \begin{bmatrix} v_1 \\ v_2 \end{bmatrix}$$

$$i_1 = y_{11}v_1 + y_{12}v_2 \qquad i_2 = y_{21}v_1 + y_{22}v_2$$

$$y_{11} = \left. \frac{i_1}{v_1} \right|_{v_2=0} \qquad y_{12} = \left. \frac{i_1}{v_2} \right|_{v_1=0} \qquad y_{21} = \left. \frac{i_2}{v_1} \right|_{v_2=0} \qquad y_{22} = \left. \frac{i_2}{v_2} \right|_{v_1=0}$$

S parameters describe the relationship of small –signal power, which are easily measured with network analyzers (VNAs):

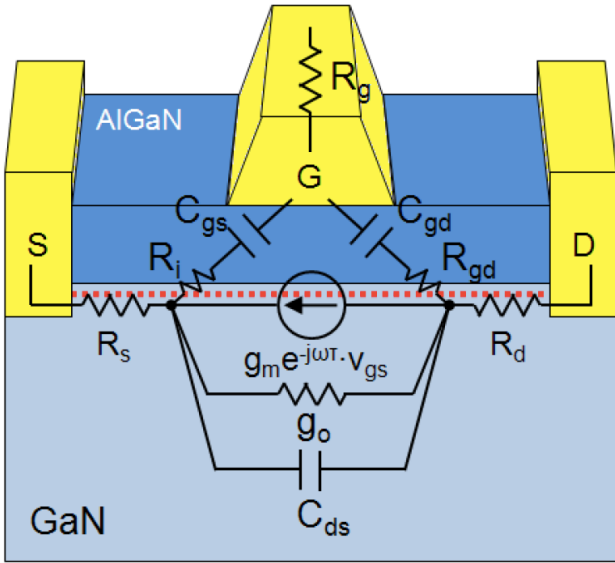
$$\begin{bmatrix} b_1 \\ b_2 \end{bmatrix} = \begin{bmatrix} s_{11} & s_{12} \\ s_{21} & s_{22} \end{bmatrix} \begin{bmatrix} a_1 \\ a_2 \end{bmatrix}$$

$$b_1 = s_{11}a_1 + s_{12}a_2 \qquad b_2 = s_{21}a_1 + s_{22}a_2$$

$$s_{11} = \left. \frac{b_1}{a_1} \right|_{\text{output match}} \qquad s_{12} = \left. \frac{b_1}{a_2} \right|_{\text{input match}} \qquad s_{21} = \left. \frac{b_2}{a_1} \right|_{\text{output match}} \qquad s_{22} = \left. \frac{b_2}{a_2} \right|_{\text{input match}}$$

The small-signal implies that the magnitude of the signal voltage is $\sim kT / q$ (~ 26 mV at $T = 300$ K):
Nonlinear characteristics of field-effect transistors can be linearized

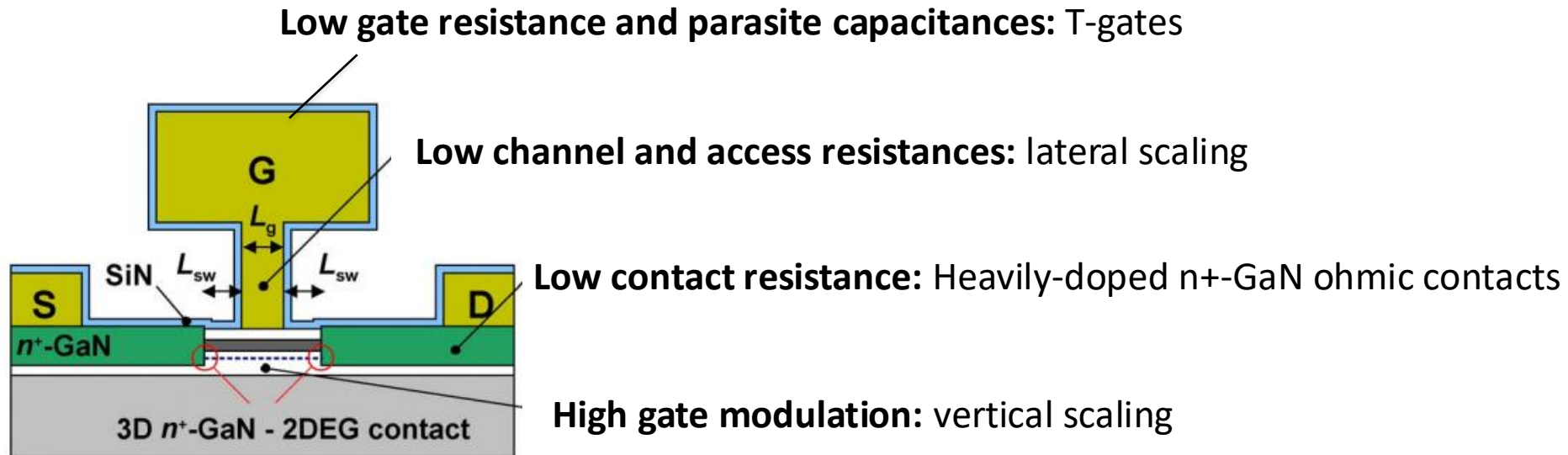
GaN RF transistors



Scaling	Material properties	Advantage
Vertical scaling	<ul style="list-style-type: none">· High DoS in GaN ($5 \times \text{InGaAs}$)· Polarization doping· High potential barrier of AlGaN	<ul style="list-style-type: none">· High vertical scalability· Thin top barrier w/ high n_s· Low gate leakage
Lateral scaling	<ul style="list-style-type: none">· High peak saturation velocity· High breakdown field	<ul style="list-style-type: none">· High $JFoM$ ($JFoM = f_T \times BV$)
Parasitic reduction	<ul style="list-style-type: none">· High n_s ($1\text{-}2 \times 10^{13} \text{ cm}^{-2}$)· High μ ($1500 \text{ cm}^2/\text{V}\cdot\text{s}$)	<ul style="list-style-type: none">· Low parasitic resistance ($\sigma = n_s \cdot q \cdot \mu$)

How to make a state of the art RF device?

RF devices: high frequency and high output power



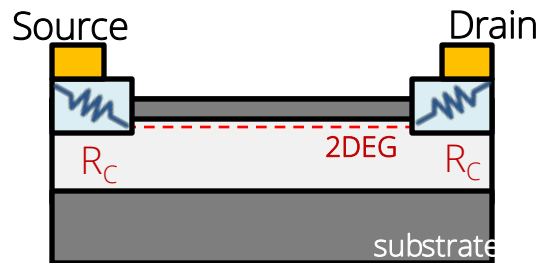
Contact resistances:

Important RC charging times are reduced by minimizing source and drain resistances and parasitic capacitances.

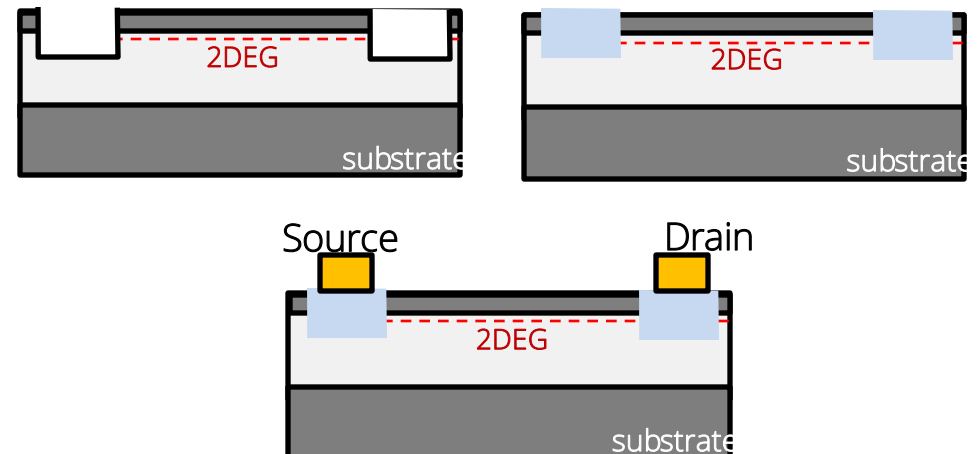
I. Conventional alloyed ohmic contacts: typically exhibit a high contact resistance of $>0.4 \text{ ohm}\cdot\text{mm}$ due to high potential barrier of AlGaIn, limiting resistance scaling.

II. Regrown n⁺GaN contacts: allows direct contact of n⁺-GaN to 2DEG and obtains an extremely low interface resistance of $0.026 \text{ ohm}\cdot\text{mm}$ because of high n_s in GaN HEMT structures [2]. A combination of high n_s and high mobility (μ) also results in a low 2DEG sheet resistance (typically, $300\text{--}400 \text{ /sq.}$) that is comparable to InGaAs HEMTs, reducing the parasitic resistance in access regions.

alloyed ohmic contacts

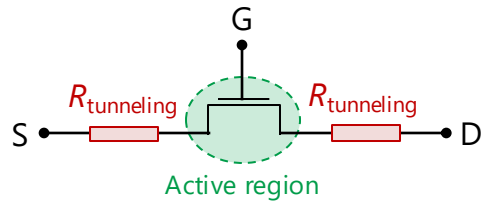
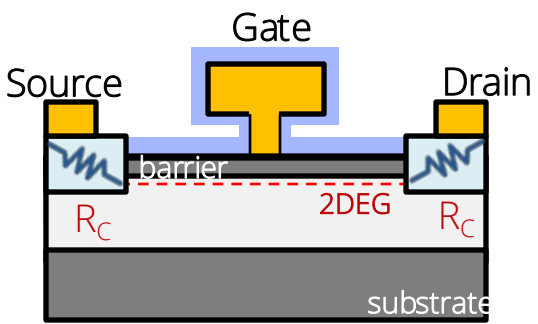


regrown ohmic contacts



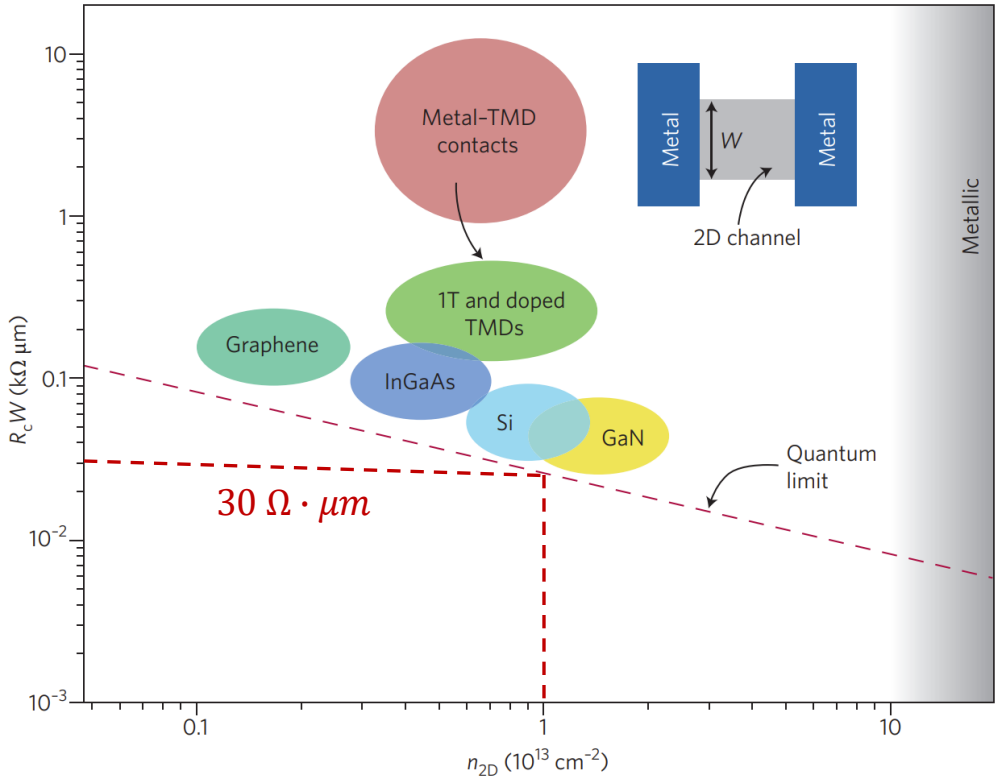
Effect of contact resistance

Contact resistance is not scalable



$R_{\text{tunneling}}^{\text{quantum-limit}} \cong 30 \, \Omega \cdot \mu\text{m}$

Resistance of a 100-nm-long semiconductor channel !



Quantum limit

$R_q = \pi h / (4q^2 k_F)$

Electron injection through metal-semiconductor contacts limits their ON-state conductance

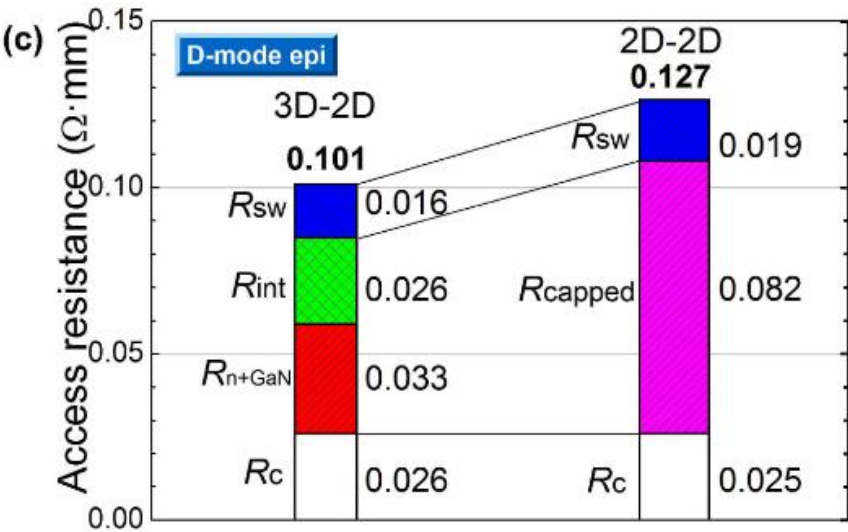
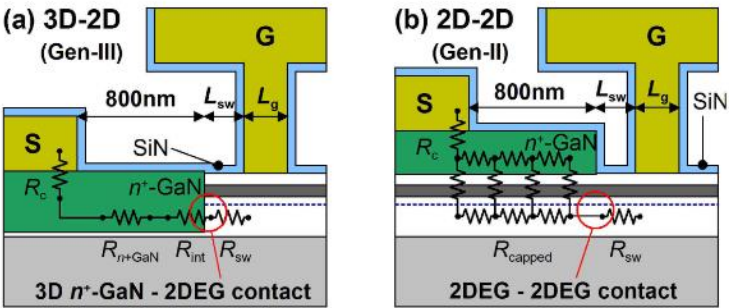
Effect of contact resistance

Contact resistances:

Important RC charging times are reduced by minimizing source and drain resistances and parasitic capacitances.

Conventional alloyed ohmic contacts: typically exhibit a high contact resistance of $>0.4 \text{ } \Omega \cdot \text{mm}$ due to high potential barrier of AlGaIn, limiting resistance scaling.

Regrown n^+ GaN contacts: allows direct contact of n^+ -GaN to 2DEG and obtains an extremely low interface resistance of $0.026 \text{ } \Omega \cdot \text{mm}$ because of high n_s in GaN HEMT structures [2]. A combination of high n_s and high mobility (μ) also results in a low 2DEG sheet resistance (typically, $300\text{--}400 \text{ } \Omega/\text{sq.}$) that is comparable to InGaAs HEMTs, reducing the parasitic resistance in access regions.

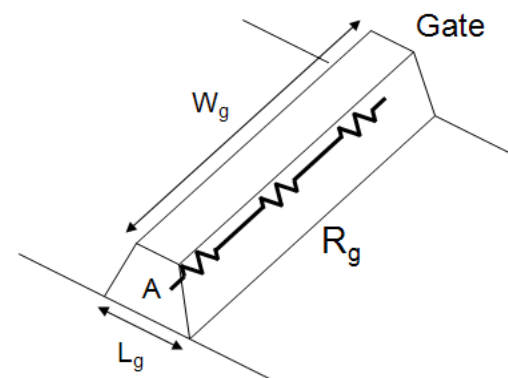
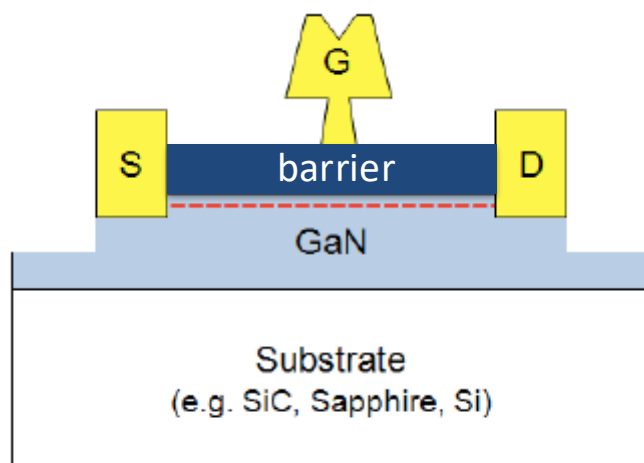


Effect of gate shape

Gate contacts: one of the most important steps for RF

- Gate modulation (g_m)
- Gate capacitances by the gate contact (C_{gs} and C_{gd})
- Gate resistance R_g to improve f_{max}

T gates



Gate resistance: $R_g \propto \rho W/A$

Small R_g requires large L_g

Gate capacitance: $C_{gd} = \frac{2\epsilon W_g}{1 + \frac{2X_{dep}}{L_g}}$

Small C requires small L_g

$$f_T = \frac{g_m}{2\pi(C_{gs} + C_{gd})(1 + (R_s + R_d)g_o) + g_m C_{gd}(R_s + R_d)}$$



$$f_{max} \cong \frac{f_T}{2\sqrt{(R_i + R_s + R_g)g_o + (2\pi f_T R_g C_{gd})}}$$

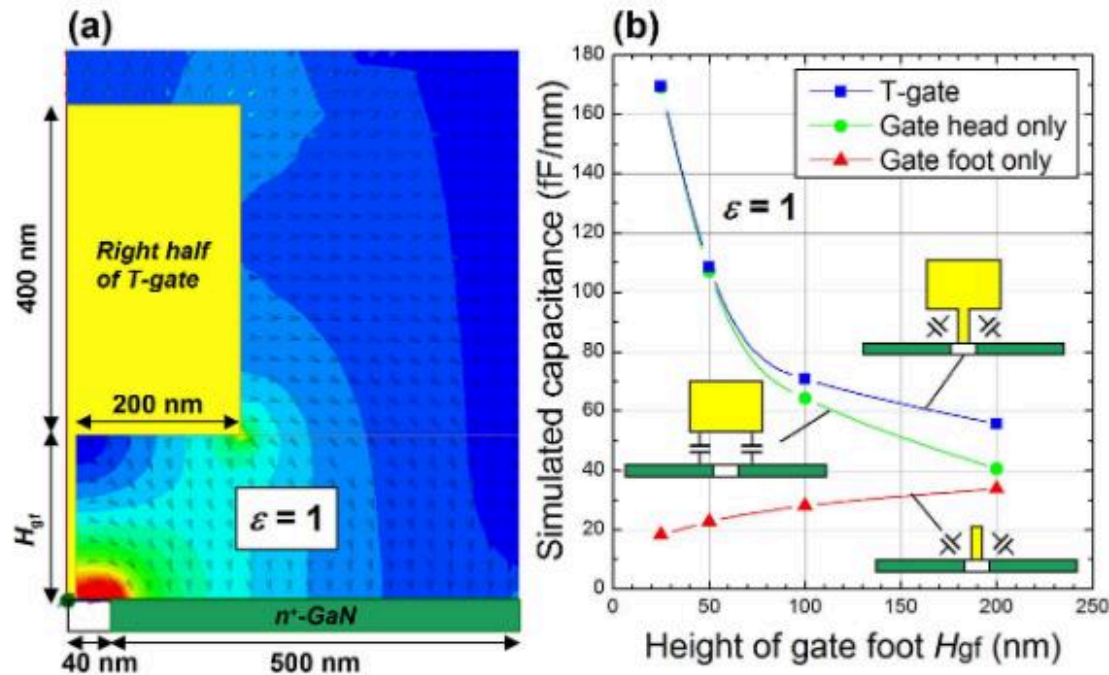


Effect of gate shape

Gate contacts: one of the most important steps for RF

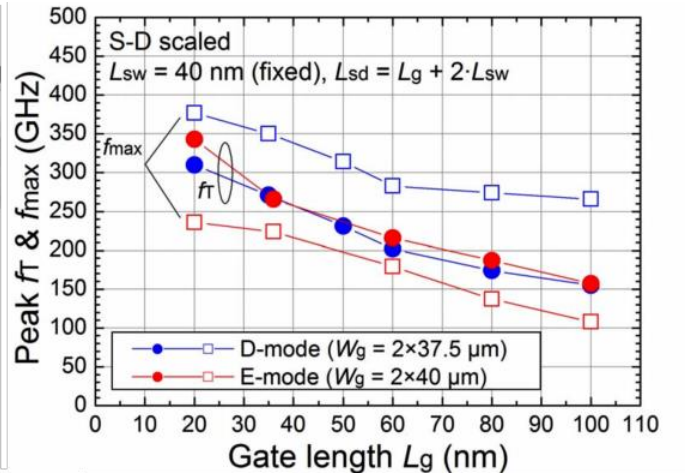
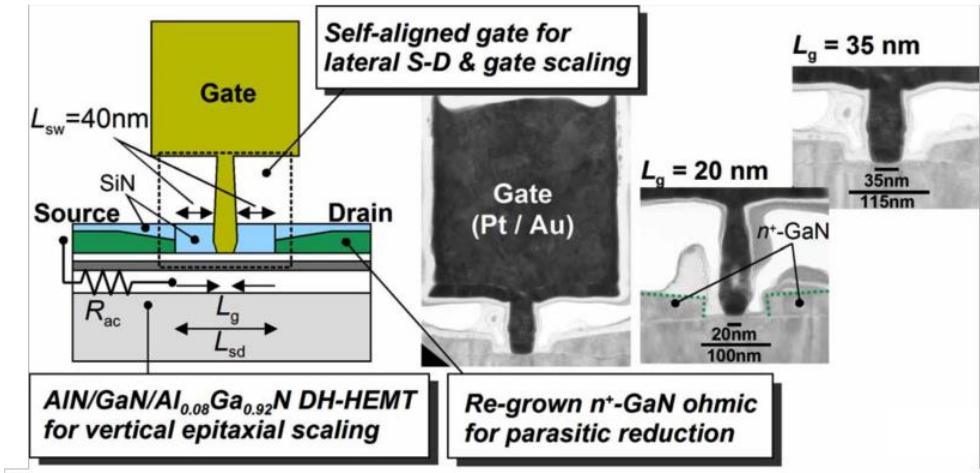
- Gate modulation (g_m)
- Gate capacitances by the gate contact (C_{gs} and C_{gd})
- Gate resistance R_g to improve f_{max}

T gates



For $H_{gf} < 100$ nm, C_p is mostly determined by the high capacitance associated with the gate head. At $H_{gf} = 200$ nm, C_p 's arising from the gate-head and the gatefoot become comparable, and a further increase in H_{gf} does not significantly reduce the total C_p .

Effect of gate shape



20-nm gate AlN/GaN/AlGa_{0.92}N double heterojunction HEMTs: $f_T/f_{MAX} = 310/364\text{ GHz}$

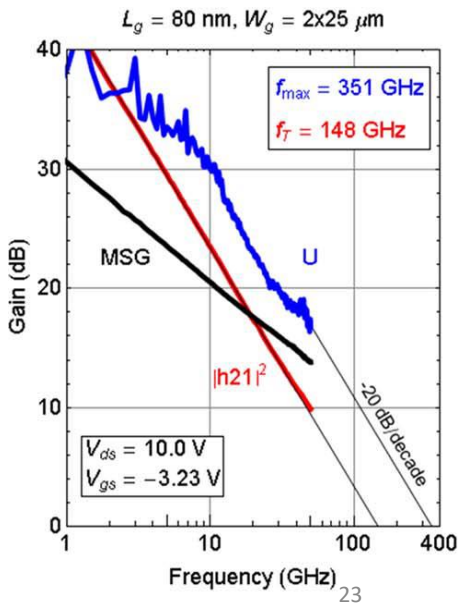
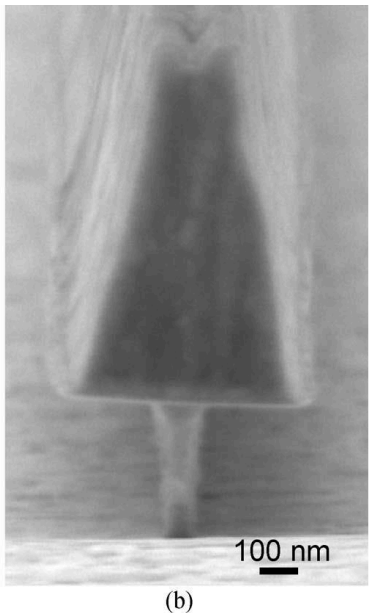
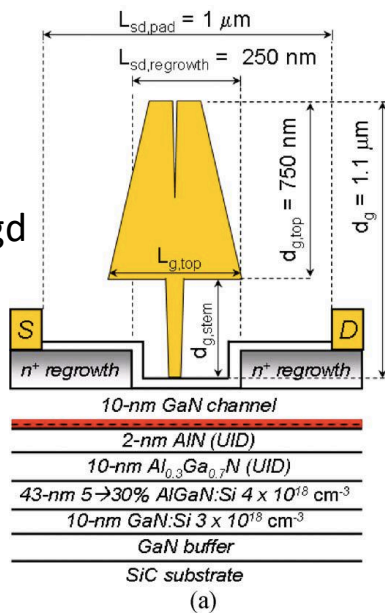
HRL laboratories: K.Shinohara et al. , IEDM 11-456 (2011).

Gates:

- 80-nm-long 1.1- μm -tall
- 370-nm-tall stem

simultaneously minimize R_g and C_{gd}

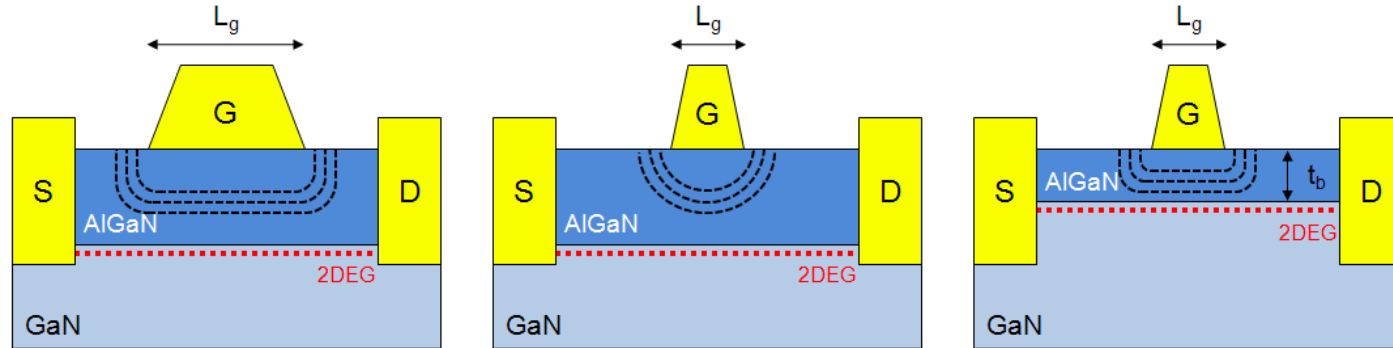
$F_{max} = 351\text{ GHz}$



Effect of barrier material

Scaling effects:

Field distribution in the channel becomes two-dimensional with both E_x and E_y : **Short channel effects**

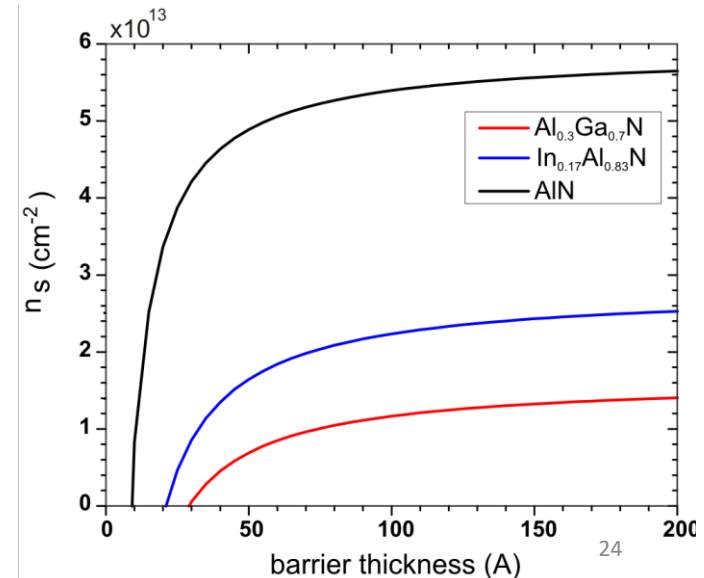


Barrier needs to be scaled accordingly $t_b \ll L_g$ but carrier density is reduced

Barrier materials with **large polarization discontinuities** allow:

- reduced barrier thicknesses
- improved gate control over electrons in the channel
- improvement in short channel effects:

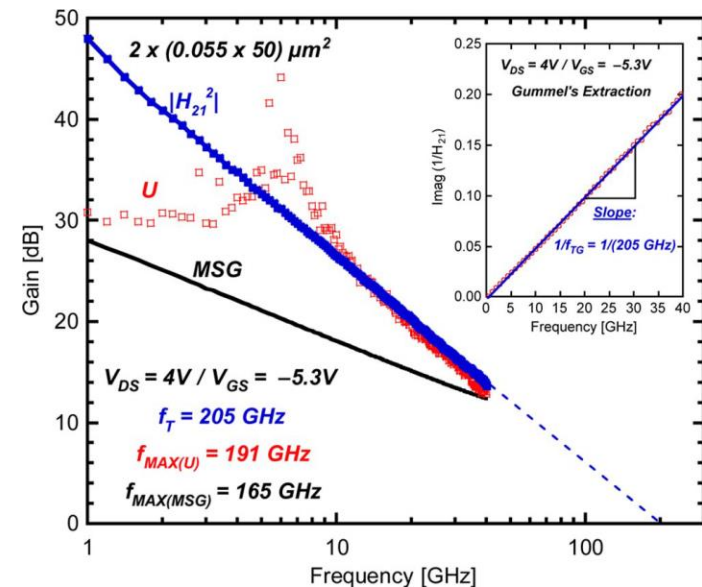
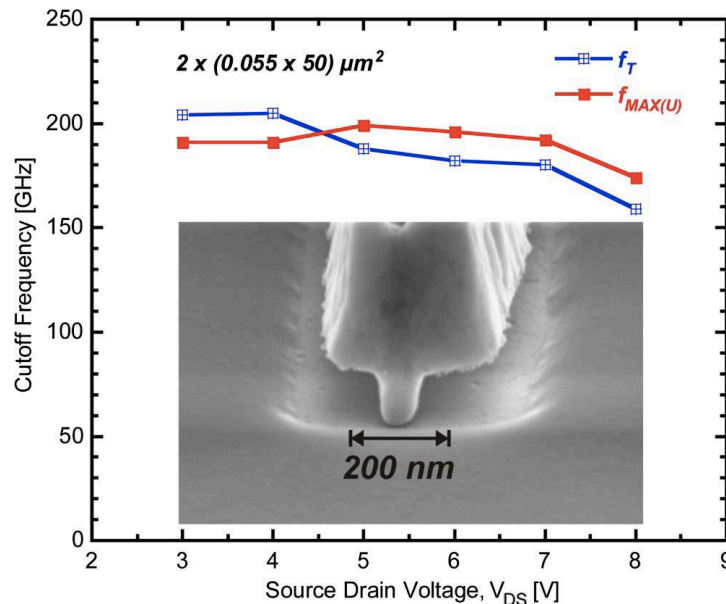
InAlN, AlN, AlInGaN, etc



Effect of barrier material

AlInN/GaN

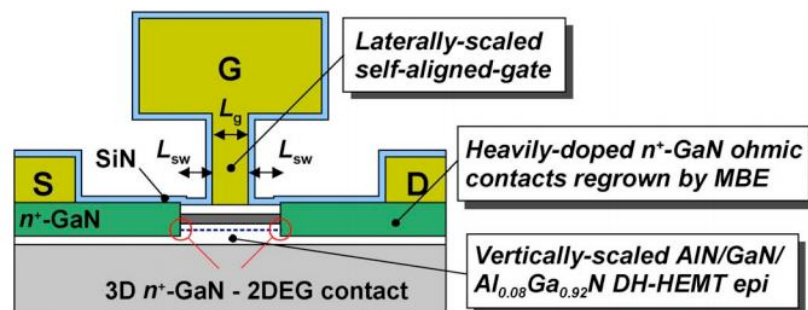
- $\text{Al}_{0.83}\text{In}_{0.17}\text{N}$ is lattice-matched to GaN
- Polarization-field discontinuity $\Delta P_0 = 2.73 \times 10^{13} \text{ ecm}^{-2}$ solely due to spontaneous polarization
in contrast to $\text{Al}_{0.2}\text{Ga}_{0.8}\text{N/GaN}$ ($\Delta P_0 = 1.18 \times 10^{13} \text{ ecm}^{-2}$) from spontaneous and piezoelectric polarization
- First proposed in J. Kuzmík, IEEE Electron Device Lett., vol.22, no.11, p.510 (2001))



- 10-nm nearly lattice-matched $\text{Al}_{0.86}\text{In}_{0.14}\text{N}$ barrier
- channel electron sheet density of $2.4 \times 10^{13} \text{ cm}^{-2}$
- mobility $\mu = 1300 \text{ cm}^2/\text{Vs}$
- gate length = 55 nm and f_T/f_{MAX} of 205/191 GHz

Effect of barrier material

AlN/GaN

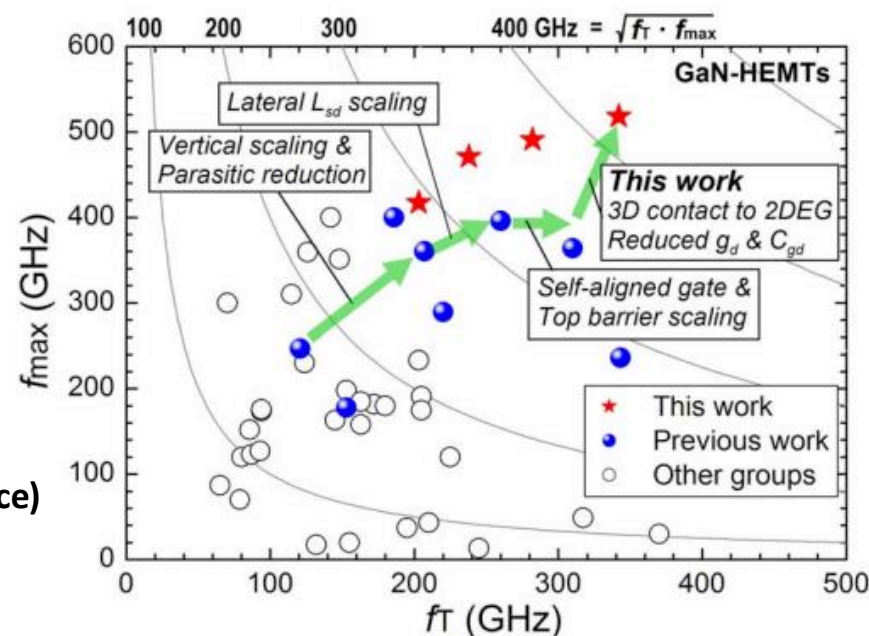


- Barrier thickness: 3.5 nm
- $n_s = 1.5 \times 10^{13} \text{ cm}^{-2}$
- **mobility (μ) of $1100 \text{ cm}^2/\text{V}\cdot\text{s}$**
- Si-doped n^+ -GaN ohmic ($7 \times 10^{19} \text{ cm}^{-3}$):
to laterally contact to 2DEG in the GaN channel
- ultra-short gate length of 20nm
- gate-source and gate-drain separation of 70nm
- f_T / f_{\max} as high up to 454/518GHz (not on the same device)
- **However, $V_{br} = 10\text{V}$**

IEEE ELECTRON DEVICE LETTERS, VOL. 36, NO. 6, JUNE 2015

Ultrahigh-Speed GaN High-Electron-Mobility Transistors With f_T/f_{\max} of 454/444 GHz

Yan Tang, Keisuke Shinohara, *Senior Member, IEEE*, Dean Regan, Andrea Corrión, *Member, IEEE*, David Brown, *Member, IEEE*, Joel Wong, Adele Schmitz, Helen Fung, Samuel Kim, and Miroslav Micovic, *Member, IEEE*



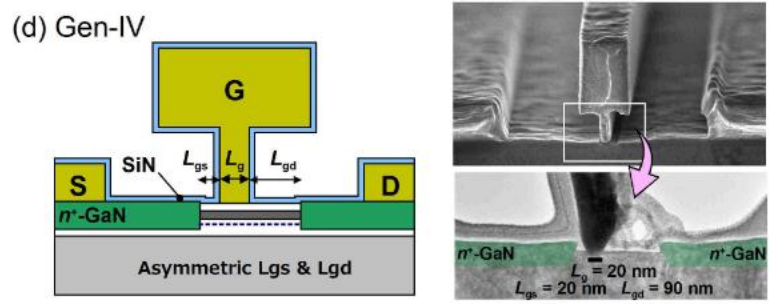
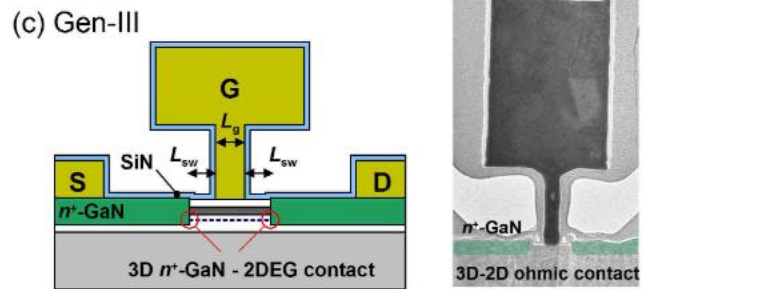
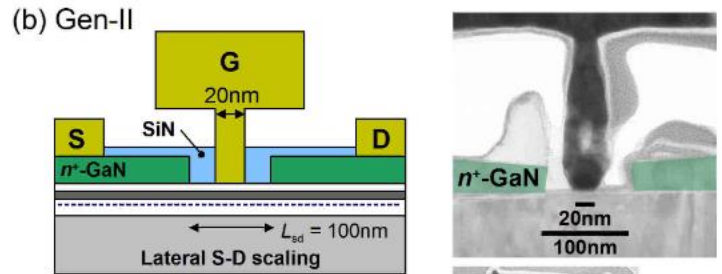
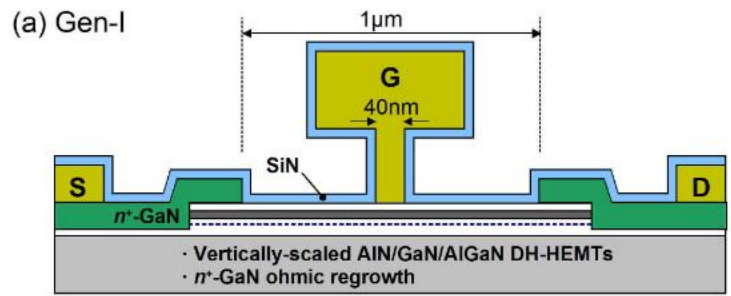
HRL laboratories:

Shinohara et al., IEDM 2011

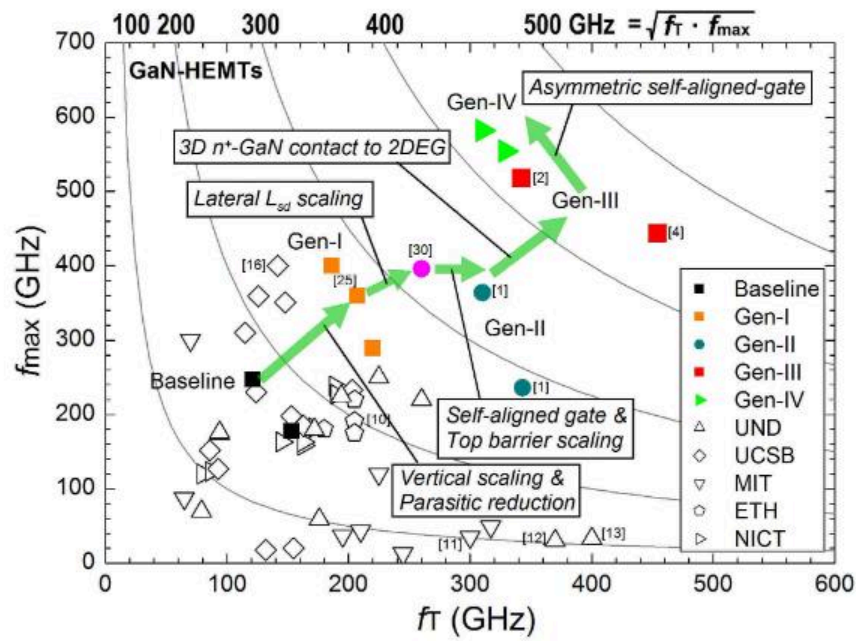
Shinohara et al., IEEE IEDM, Dec. 2012

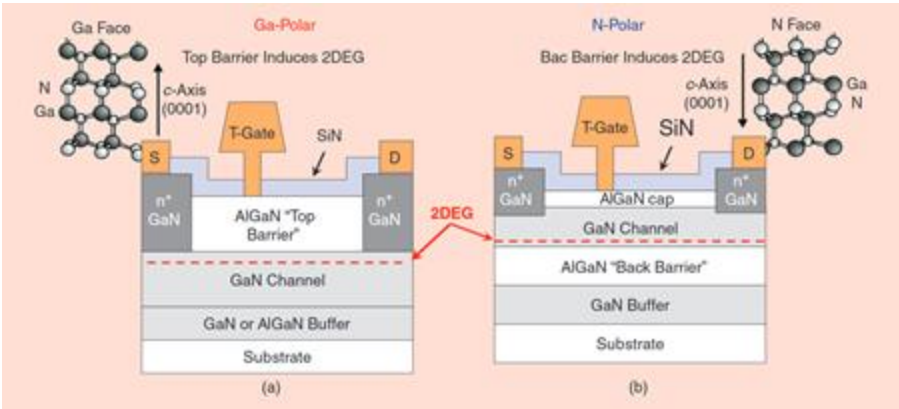
Tang et al., IEEE ELECTRON DEVICE LETTERS, VOL. 36, NO. 6, JUNE 2015

AlN/GaN

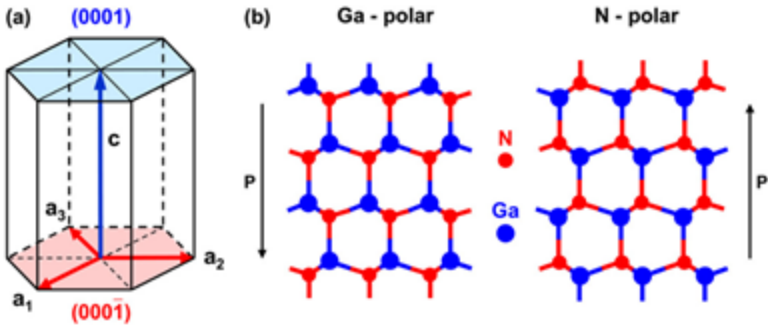


Scaling generation	Specific features
Gen-I	<ul style="list-style-type: none">Vertically-scaled AlN/GaN/AlGaN DH-HEMT epi structureLow resistance n+-GaN ohmic regrowth
Gen-II	<ul style="list-style-type: none">Lateral S-D scaling using self-aligned-gate technologySuppressed drain delay & velocity enhancement
Gen-III	<ul style="list-style-type: none">Direct contact of 3D n+-GaN ohmic to 2DEGReduced Ron and enhanced electron supply (Idmax, gm)E/D-mode integrated DCFL ring oscillators
Gen-IV	<ul style="list-style-type: none">Asymmetric self-aligned-gate technologyIncreased BV and reduced short-channel effect (DIBL, fmax)Low noise characteristics at low power

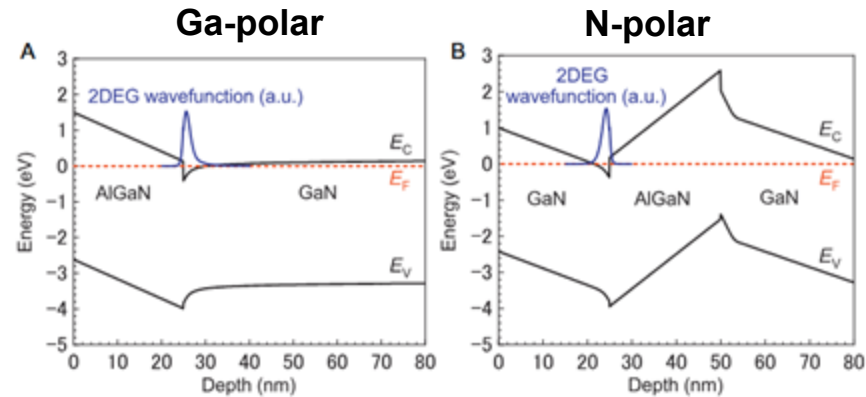




F. Medjdoub et al., IEEE Microwave Magazine (25), 10, 2024



S. Keller et al., 2014 Semicond.Sci.Technol. 29 113001

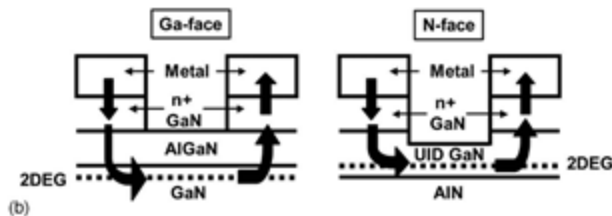


M. H. Wong et al., Semiconductors and Semimetals, Volume 102, 2019 Elsevier Inc

- **Ga-polar:** the 2DEG channel is between below the AlGaN top barrier
- Problem:** tradeoff between high current density and scalability
- **N-polar:** the 2DEG is underneath the GaN channel

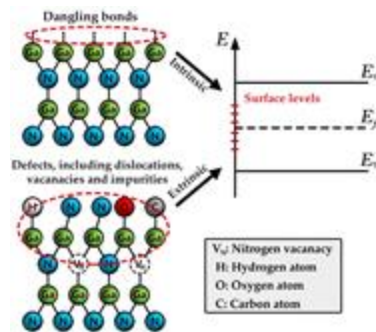
N-polar GaN

- **Scalability** without penalty on the 2DEG density
- **Lower resistance** ohmic contacts

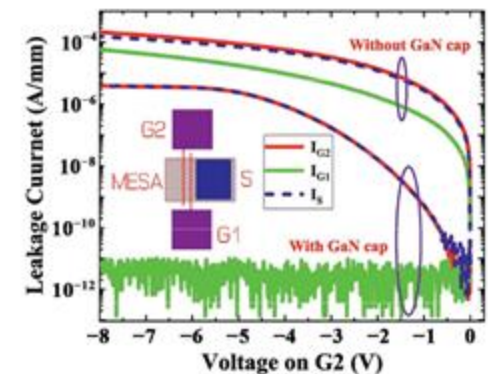
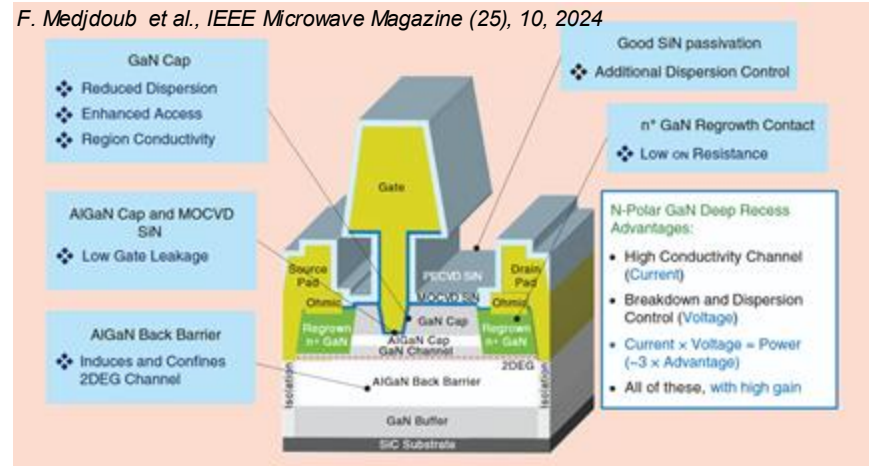


M. H. Wong et al., *APPLIED PHYSICS LETTERS* 91, 232103 2007

- **Deep-recess GaN cap**: effective in situ passivation layer for surface defects which act as a “virtual gate”



Pengfei Zhu et al., *Crystals* 2022, 12, 1461

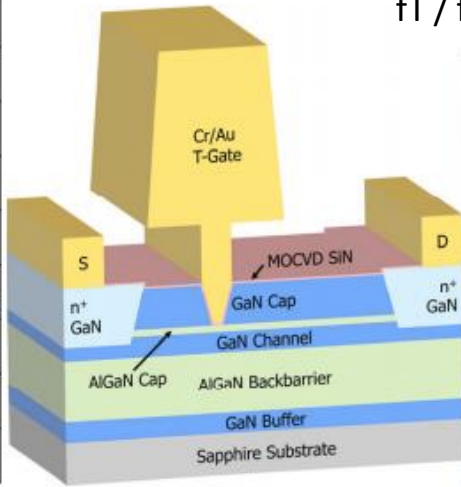


N-polar GaN

Reversed polarization fields of N-polar GaN/Al(In,Ga)N offers

- improved electron confinement
- flexibility to scale the gate-to-2DEG distance without changing the charge density in the 2DEG.
- Ultra low contact resistance values since the contacts are not made through a high band-gap barrier ($\sim 30 \Omega\mu\text{m}$)
- improved gate-channel distance scalability
- Improved breakdown voltage

22 nm GaN Cap
2.6 nm $\text{Al}_{0.27}\text{Ga}_{0.73}\text{N}$ Cap
10 nm GaN Channel
0.7 nm $\text{Al}_{0.48}\text{Ga}_{0.52}\text{N}$
10 nm $\text{Al}_{0.32}\text{Ga}_{0.68}\text{N}$
20 nm graded $\text{Al}_x\text{Ga}_{1-x}\text{N}:\text{Si}$ x: 5 to 32% [Si] = $5 \times 10^{18} \text{ cm}^{-3}$
10 nm GaN:Si [Si] = $5 \times 10^{18} \text{ cm}^{-3}$
GaN:Fe Buffer
Sapphire Substrate



$$f_T / f_{\text{max}} = 148/330\text{GHz}$$

